An enhanced approach to virtually increase quasi-stationarity regions within geometric channel models for vehicular communications

Fidel Alejandro Rodríguez-Corbo, Mikel Celaya-Echarri, *Member, IEEE*, Raed M. Shubair, *Senior Member, IEEE*, Francisco Falcone, *Senior Member, IEEE*, and Leyre Azpilicueta, *Senior Member, IEEE*

***Abstract*—Vehicular communication channels are intrinsically non-stationary, as they present high mobility and abundant dynamic scatterers. Quasi-stationary regions can assess the degree of non-stationarity within a determined scenario and time variant observation of the channel can be extracted. These regions can aid geometrical models as to increase channel sampling intervals or to develop hybrid stochastic-geometric channel models. In this work, a new methodology for the use of virtual quasi-stationary regions within geometric channel models is proposed, in order to leverage the inherent location information to virtually increase their size. Overall, the use of delay-shifted channel responses improves the mean correlation coefficient between consecutive locations, ultimately reducing computation time for time-variant geometric channel models.**

***Index Terms*—Non-stationarity, 3D Ray-Launching, correlation matrix, quasi-stationarity regions, geometric channel models, V2X.**

I. Introduction

EFFICIENT and reliable vehicular communications is of utmost significance within Intelligent Transportation Systems (ITS), as the practical use of these networks will improve by several orders the security and capabilities of the transportation infrastructure as we know it nowadays. One characteristic that may not be always fulfilled for a vehicular channel is the wide-sense stationary and uncorrelated scattering (WSSUS) assumption. Although in the past this assumption has proven very useful, the extreme conditions in vehicular communication (V2X) channels and the adoption of higher carrier frequencies like millimeter wave (mmWave) may predict erroneous statistics with this simplification. In the literature, it has been widely referenced that this assumption is only valid for a short period of time and frequencies [1]–[4]. On top of this simplified depiction of the wireless channel, many important algorithms rely on the use of second-order statistics to set functionalities and parameters [5]. Due to this non-WSS behavior of V2X channels, a method to obtain the statistics needed is to estimate the quasi-stationary regions (QSRs) where the channel is considered to be similar enough that the statistics can be assumed to be stationary within them. In this regard, some methods as to how to assess the degree of non-stationarity have been put forward, where most of them revolve around correlation metrics and spectral divergences typically applied to the power-delay-profile (PDP), shadow fading, local scattering function (LSF), or some other time/location evolutionary channel characteristic. Some of these methods are well tailored to multiple-input-multiple-output (MIMO) systems like the correlation matrix distance (CMD) found in [6]–[8] , and for single-input-single-output (SISO) systems, power correlation methods are a frequent choice [9]–[11]. Another utility for the QSRs comes in the form of deterministic simulation sampling for non-stationary conditions. Geometrical deterministic models usually have to sample transceivers' position as low as $\lambda/2$ wavelength in Monte Carlo simulations in order to replicate movement. This is especially true in deterministic models like Ray Tracing/Launching (RT/L) where the number of simulations as well as the corresponding computational cost can be intractable or unmanageable when considering mmWave simulations in dynamic conditions for complex outdoor high-dense heterogeneous scenarios. In this sense, acceleration schemes have been proposed, from the hardware standpoint using GPU acceleration [12], software based on smart tracing [13] or ray selection criteria [14]. In some cases, interesting applications like real-time RT for directional characteristics estimations of the channel has been proposed [15], although still highly computationally intensive. In the case of spatial sampling, acceleration techniques have been proposed based on quasi stationary distances [11], [16], reducing the number of simulations needed by increasing the spatial sampling distances to accelerate the RT simulations of a vehicular environment. In general, the use of QSRs within deterministic models can aid not only in the sampling interval but also can be the integration point with hybrid models, that can use the quasi-stationarity condition to fill the blanks with a stochastic channel response generator. In this context, QSRs can leverage the advantages of a deterministic setup, in which the complete discrete geometrical information is known, and therefore, it can be used to virtually increase QSRs in the simulator, for optimization purposes. Following this approach, in this work, a further step is proposed, introducing a novel technique for the use of virtual

The authors wish to acknowledge the support received from Grant No. RYC2021-031949-I, funded by MCIN/AEI/10.13039/501100011033 and NextGenerationEU/PRTR, and Project PID2021-127409OB-C31, funded by MCIU/AEI/FEDER, UE. (*Corresponding author: Leyre Azpilicueta*)

L. Azpilicueta and F. Falcone are with the Electric, Electronic and Communication Engineering Department and the Institute of Smart Cities, Public University of Navarre (UPNA), Spain. (E-mail: leyre.azpilicueta@unavarra.es).

F. A. Rodríguez-Corbo and F. Falcone are with the School of Engineering and Sciences, Tecnologico de Monterrey, Mexico.

M. Celaya-Echarri is with the Department of Statistics, Computer Science and Mathematics, Public University of Navarre (UPNA), 31006, Pamplona, Spain.

R. M. Shubair is with the Department of Electrical and Computer Engineering, New York University Abu Dhabi, Abu Dhabi 129188, UAE.

Manuscript received April, 2023; revised XX, 2023.

QSRs (vQSRs) within deterministic channel simulators with delay-shifted channel responses. The delay shift is distance dependent and can always be recovered by leveraging the coordinate system within deterministic methods. This modification can increase the correlation between distance/time lags of the PDPs, and consequently, significantly reduce simulation cost. The proposed method can be generalized for all geometric deterministic approaches.

The remaining parts of this letter are organized as follows: Section II describes the methodology to virtually enhance QSRs within geometric channel models. Section III describes the 3D-RL implementation as well as the considered generic scenario. Results and discussion with the comparison of the correlation matrices and mean correlation are outlined in Section IV. Finally, conclusions are presented in Section V.

II. Methodology

V2X communication channel characteristics can change considerably within a short period of time due to the movement of the transceivers and/or the effective scatterers, rendering it non-stationary. A correlation of the time-dependent channel response power profile can be calculated, in order to quantify the channel non-stationarity degree. In [10], a definition of the temporal PDP correlation coefficient (TPCC) for time lag representation is presented, but it can also be translated to location and distance lag conditioned, which is a representation of most utility for geometrical models. Using a position-relative representation and a discretization of the PDP, Equation (1) shows the position-indexed discrete TPCC.

$$\rho(i,j) = \frac{\sum_{n=0}^{N-1}(\overline{P}(i,n\Delta\tau) * \overline{P}(j,n\Delta\tau))}{max\{\sum_{n=0}^{N-1}(\overline{P}(i,n\Delta\tau)^2), \sum_{n=0}^{N-1}(\overline{P}(j,n\Delta\tau)^2)\}} \tag{1}$$

Where $\rho(i,j)$ is the correlation coefficient, i and j are the position index of the receiver using Δr as the unit of displacement between consecutive positions, $\overline{P}(i/j,n\Delta\tau)$ is the average PDP (APDP) at the indexed position, and n is the delay index from 0 to $N-1$, where N is the maximum delay cap of the model divided by the delay resolution $\Delta\tau$. The APDP is obtained by averaging the instantaneous channel response using a sliding window in the position indexed (can also be translated to time) domain as follows:

$$\overline{P}(i,n\Delta\tau) = \frac{1}{W}\sum_{i}^{i+W-1}|h(i,n\Delta\tau)|^2 \tag{2}$$

Where W is the length of the sliding window, and $h(i,n\Delta\tau)$ is the channel response at the indexed position. The correlation approach of Equation (1) is strongly dependent on delay interrelation within the correspondence delay bin. A mismatch of nearly identical multi-path contribution can result in a considerable decrease in the correlation coefficient, and as a result a cease in the QSR condition. This delay drift of the multi-path and the line-of-sight (LOS) contributions are associated with the distance changes between the transceivers, and from the perspective of geometric modeling the relative locations of the transceivers are always known. Thus, the distance dependent delay for LOS contributions has its lower delay limit in the propagation time between transceivers as follows:

$$\tau_{iLOS} = \frac{\mathbf{d_{iLOS}}}{c_0} \tag{3}$$

Where c_0 is the speed of light in vacuum and d_{iLOS} is the LOS distance. This information is already embedded in the channel geometrical information and can be extracted from the channel response at no information lost. Typically, geometric models depict transceivers' and scatterers' positions using a general coordinate reference, where relative distances can be extracted for each location in the selected simulation. Fig. 1 shows a 3D cartesian framework where vectorized locations for the transceivers are used.

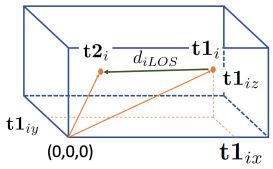

Fig. 1: Schematic view of the 3D cartesian framework used to designate the vectorized position of the transceivers.

Within this description of the coordinates, the relative distance between transceivers can be obtained using Equation (4).

$$d_{iLOS} = ||\mathbf{t2}_i - \mathbf{t1}_i||, \quad \texttt{where} \quad \mathbf{tk}_i = [\mathbf{tk}_{ix} \;\; \mathbf{tk}_{iy} \;\; \mathbf{tk}_{iz}]^T \tag{4}$$

Where $||\cdot||$ is the 2-norm and $\mathbf{tk}_i$ is the $k-th$ transceiver's position at indexed instant/position i, in vector form. This LOS distance can then be used to calculate the τ_{iLOS} delay in the specific locations of the selected simulation and a new delay-shifted channel response can be obtained. Assuming that is a virtual depiction of the channel response, where the delay-shift correction is within the channel geometrical information, it can be named as a virtual channel response, represented in Equation (5). A trace back to the real channel response is position dependent and can be regain at any instant.

$$h_v(i,n\Delta\tau) = h(i,(n\Delta\tau + \tau_{iLOS})) \tag{5}$$

Overall, delay-shifted virtual responses maintain invariant the scatterers distribution dispersions, taking into account a constant displacement of the power profile. This change consequently increases the correlation of power between consecutive PDP, as it eliminates the drift of the distance dependent LOS propagation delay for all components. The virtual channel response from Equation (5) can be used for the APDP in Equation (2) and furthermore in the TPCC in order to virtually enhance real QSRs, increasing their size as new vQSRs, without information lost. It must be remarked that this new obtained vQSRs representation is only for simulation purposes and it should not be interpreted as real QSR within the current scenario. The main objective of the use of vQSRs is to remove duplicated information within the modeling technique, that is the distance dependent propagation delay, in order to increase the correlation coefficient within consecutive locations (or time). This increase in vQSRs can be used to enhance the channel model sampling technique reducing computational cost, or to develop new optimized hybrid stochastic-geometric channel models, considering that for every use, ultimately, the channel response must be corrected by inversing Equation (5).

III. 3D-RL Implementation

The previous described methodology has been implemented in an in-house developed deterministic RL algorithm in order to analyze in deepness real QSR and their corresponding increased vQSRs within a real generic vehicular scenario, for simulation optimization purposes. The RL technique is a geometry-based deterministic model (GBDM) which considers the three-dimensional (3D) morphology and topology of the complete scenario, as well as all the transceivers and scatterers within it, with their corresponding material properties (conductivity and relative permittivity) at the selected system operating frequency. Its principle is based on geometrical optics (GO). To complement the GO theory, the diffracted rays are introduced with the Geometrical Theory of Diffraction (GTD) and its uniform extension called as the uniform GTD (UTD). In addition, electromagnetic phenomena such as reflection, refraction or diffraction are considered as well. Finally, parameters such as the operating frequency, number of ray reflections, type of antenna, or angular and spatial resolution, are established before simulation. Following this technique, accurate large and small-scale parameters can be obtained for all the spatial/volumetric locations of the considered scenario. A detailed description of the 3D-RL algorithm can be found in [17], [18], and its validation for complex vehicular environments at the mmWave spectrum is presented in [19], [20]. In this work, the proposed methodology has been applied to a generic complex urban high-dense vehicular scenario for non-stationarity vQSR regions simulation validation purposes. Nevertheless, this technique can be implemented to any particular scenario, without loss of generality and regardless the geometric simulator used. Fig. 2 presents the schematic view of the recreated scenario for simulation. It corresponds to a central city avenue with two directions and a median with inhomogeneous vegetation, surrounded by a 2 m sidewalk and medium and high tall buildings on the sides. A high density of vehicles has been considered, with a total of 18 vehicles constantly driving along the road, emulating rush hour. The transmitter (TX) has been placed as a road-side unit (RSU) in the sidewalk at 2 m height and the receiver (RX) has been considered just above the roof of the first vehicle on the opposite road to the TX. Both locations as well as the vehicle movement are depicted in Fig. 2. Following Ref. [3], the unit of displacement Δr in the movement's direction has been set as 10λ (approx. 0.1 m) and a sliding window of four steps (40λ) has been used to calculate the APDPs in Equation (2). Simulation parameters are presented in Table I.

TABLE I: 3D-RL SIMULATION SETUP PARAMETERS

Simulation Parameters	Value
Frequency/Bandwidth	28 GHz/Carrier
TX/RX Antenna Type - Gain	Omnidirectional-3 dBi
TX/RX Antenna Height	2 m/1.5 m
TX power/RX LNA	24 dBm/27 dBi
3D-RL Angle (ϕ, θ)/Delay $\Delta\tau$ Resolution	(0.5º, 1º)/2.5 ns
Number of reflections/Diffraction	4/Yes
Scenario Dimensions/Unit of displacement Δr	(50x68x17) m/0.1 m

IV. Results and Discussion

The correlation matrices for the receiving vehicle have been calculated considering the real channel response and the virtual delay-shifted channel response, for evaluation purposes. Fig. 3 (left) shows the correlation matrix calculated from the original channel response using Equation (1) and Fig. 3 (right) presents the correlation matrix when the delay-shifted channel response from Equation (5) is employed. Both correlation matrices represent every location (434 Δr) along the effective RX trajectory (43.4 m) in the considered scenario.

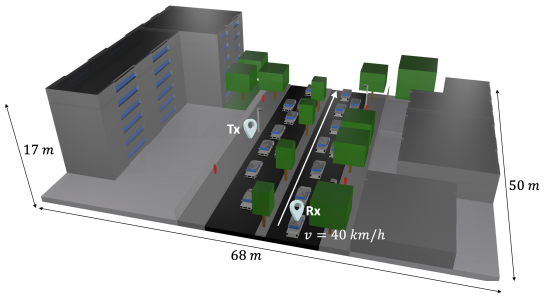

Fig. 2: Schematic view of the considered urban scenario in the 3D-RL algorithm, with the TX and RX locations and the vehicle movement direction.

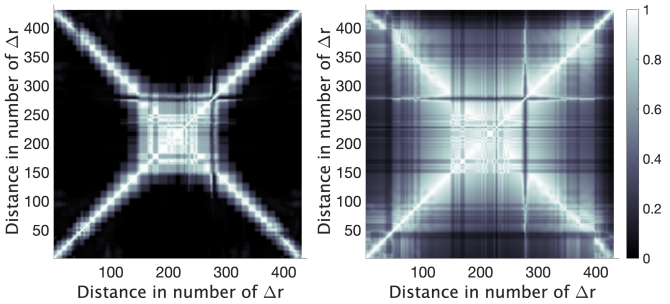

Fig. 3: Correlation matrices calculated with the original channel response (left) and with the delay-shifted channel response (right).

From Fig. 3, it is worth noting the symmetry effect that arises from the scenario disposition. The TX is located center stage, with equidistant positions for opposed vehicle locations within the route. This behavior highlights the correlation coefficient effect of delay-distance coherence between far-off locations, upscale in mmWave bands, as most of the energy contributions comes from LOS and first-order multi-path propagation. This effect can also be evidenced at the tail end of Fig. 5 (which is introduced later), with the mean correlation versus distance lags. Overall, this relationship is site-specific and determined by the considered scenario distribution and its mostly LOS conditions prevalence, but for other environments and scenarios can be radically different. As seen from Fig. 3 (right), the broad correlation coefficient has increased compared with the one in Fig. 3 (left). Further distance lags can attain higher correlation as LOS component are mostly aligned within the same bin resolution, and distance drift has been removed from the channel response.

In order to visualize the delay-shift of the time-variant APDP using the original or the virtual channel response, Fig. 4 shows the time-variant APDP comparison for the last 13.4 m section of the trajectory, approximately 1.2 seconds. From the non-shifted channel response, LOS component is moving further away in delay time, as these are the last

meters of the path. After LOS components, it can be observed some strong contributions from distance consistent scatters, following LOS drift. These distant-consistent scatters are other traveling vehicles (constant 40 km/h velocity is used for all vehicles) along the avenue, but they can also be different recurrent scatters with relative constant distance to the RX. The latter, and considering vehicular communications, can also be surrounding street side buildings, as these elements can contribute as mostly constant distance scatter from the roadside TX point of view. Moreover, two strong non-distance consistent contributions are also observed, one getting closer to the RX and the other going away. These contributions can be probably explained by the metallic fence, placed along the roads. Overall, from the delay-shifted channel response of Fig. 4, it is clearly observed that LOS components fall within the first bins. Considering mmWave conditions, most of the energy contributions comes from these components, subsequently increasing the correlation coefficient. Furthermore, distance-consistent contributions are also aligned within near shifted delays as they follow the LOS drift, likewise adding to the channel response correlation. Otherwise, as non-distance consistent scatters do not drift in time parallel to the LOS, they do not contribute with high impact to the new estimation of the channel correlation coefficient.

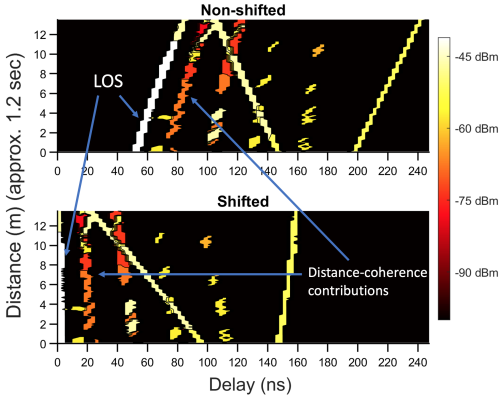

Fig. 4: Time-variant APDP using the original (non-shifted) and the virtual (delay-shifted) channel response.

Finally, the mean correlation coefficient versus distance (although it can also be calculated in time) lag has been calculated and presented in Fig. 5, considering the original channel response and the delay-shifted channel response, allowing QSR and vQSR comparison. The length of the region is determined as the distance between full correlation coefficient up to a threshold selection. Therefore, the threshold selection is pivotal in order to determine precisely the characterization criteria where quasi-stationarity is considered, and thus, the length of the region. In this study, three of the most typically used thresholds: 0.9, 0.8 and 0.7, have been considered to assess the vQSR correlation increase under several threshold selections [9], [16], [21].

There is an overall increase in the mean correlation coefficient above the one computed from the non-shifted channel response. For low lag distances this effect is not as noticeable as for larger distances lags, due to the low time delay drifts that occur within short distances lags. This was an expected result

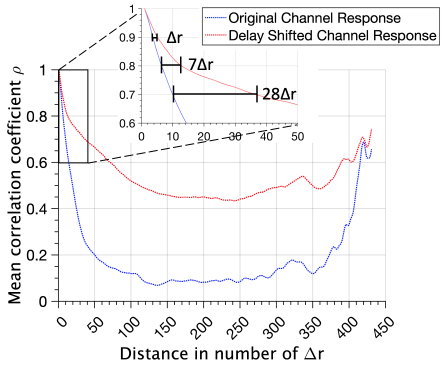

Fig. 5: Linear distribution of the mean correlation coefficient versus distance calculated with the original channel response and the delay-shifted channel response in the considered scenario.

as the mean correlation coefficient for real channel responses captures this slow drift of power contributions within the same delay bin to assess channel QSR. For larger distance lags, the decorrelation does not come from delay differences in the channel response only, but mostly related to power decay/rise and/or scatters distributions resulting in the appearance and disappearance of multi-path contributions. The effect of the tail of Fig. 5 is related with the symmetry effect shown in Fig. 3, which is site-specific and depends on the scatterers scenario disposition. From the obtained results, the regions' length increases from $4\Delta r$,$6\Delta r$, and $10\Delta r$ (equivalently to 0.4, 0.6, and 1 m) for thresholds of 0.9, 0.8, and 0.7, respectively, in the QSR case, to $5\Delta r$,$13\Delta r$, and $38\Delta r$ (equivalently to 0.5, 1.3, and 3.8 m) for the same thresholds, in the vQSR case. Overall, the increase in distance is noticeable, especially for lower thresholds like 0.7 where less correlation restriction can sum up to more than three times the distance. Table II shows a summary of the selected mean correlation coefficients as well as their corresponding vQSR increase and computational cost decrease.

TABLE II: vQSR INCREASE AND COMPUTATIONAL COST DECREASE

Mean TPCC	QSR (in meters)	vQSR (in meters)	Length increase (%)	Computational decrease (%)
0.9	0.4	0.5	25	20
0.8	0.6	1.3	216.7	54
0.7	1	3.8	380	72

V. Conclusion

In this work, a new vQSR methodology within geometric models is proposed for simulation optimization. The use of delay-shifted channel responses based on LOS propagation delay, can increase the mean correlation coefficient between consecutive RX locations. The application of this specific implementation in a generic complex urban vehicular scenario gives rise to a 25, 216, and up to 380% vQSR increase and a 20, 54 and 72% computational cost decrease, from the original QSR, both considering the same thresholds of 0.9, 0.8, and 0.7 respectively. These results and the proposed vQSR technique can aid in a simulation enhancement for time-variant geometric channel models, as to be used for sampling distances or for hybrid geometric-stochastic channel models, ultimately reducing computational cost.

REFERENCES

[1] M. Yusuf, E. Tanghe, F. Challita, P. Laly, D. P. Gaillot, M. Lienard, L. Martens, and W. Joseph, "Stationarity Analysis of V2I Radio Channel in a Suburban Environment," *IEEE Trans. on Veh. Tech.*, vol. 68, no. 12, pp. 11 532–11 542, Dec. 2019.

[2] L. Bernado, T. Zemen, F. Tufvesson, A. F. Molisch, and C. F. Mecklenbrauker, "The (in-) validity of the WSSUS assumption in vehicular radio channels," in *2012 IEEE 23rd Int. Symp. on Personal, Indoor and Mob. Radio Comms. - (PIMRC)*, Sep. 2012, pp. 1757–1762.

[3] R. He, O. Renaudin, V.-M. Kolmonen, K. Haneda, Z. Zhong, B. Ai, and C. Oestges, "Characterization of Quasi-Stationarity Regions for Vehicle-to-Vehicle Radio Channels," *IEEE Trans. on Ant. and Prop.*, vol. 63, no. 5, pp. 2237–2251, May 2015.

[4] L. Azpilicueta, C. Vargas-Rosales, F. Falcone, and A. Alejos, *Radio Wave Propagation in Vehicular Environments*. SciTech Publishing, 2020.

[5] A. Ispas, G. Ascheid, C. Schneider, and R. Thoma, "Analysis of Local Quasi-Stationarity Regions in an Urban Macrocell Scenario," in *2010 IEEE 71st Veh. Tech. Conf.*, May 2010, pp. 1–5.

[6] R. He, O. Renaudin, V. M. Kolmonen, K. Haneda, Z. Zhong, B. Ai, S. Hubert, and C. Oestges, "Vehicle-to-Vehicle Radio Channel Characterization in Crossroad Scenarios," *IEEE Trans. on Veh. Tech.*, vol. 65, no. 8, pp. 5850–5861, Aug 2016.

[7] J. Y. Hong, C.-S. Kim, J.-S. Lim, and H.-J. Kim, "Non-stationarity of vehicle to vehicle channels using correlation or covariance in highway scenarios," in *2018 Int. Conf. on Inf. and Comm. Techn. Convergence (ICTC)*, Oct 2018, pp. 1546–1548.

[8] O. Renaudin, V.-M. Kolmonen, P. Vainikainen, and C. Oestges, "Non-Stationary Narrowband MIMO Inter-Vehicle Channel Characterization in the 5-GHz Band," *IEEE Trans. on Veh. Tech.*, vol. 59, no. 4, pp. 2007–2015, May 2010.

[9] F. Li, W. Chen, and Y. Shui, "Analysis of Non-Stationarity for 5.9 GHz Channel in Multiple Vehicle-to-Vehicle Scenarios," *Sensors*, vol. 21, no. 11, p. 3626, May 2021.

[10] R. Wang, C. U. Bas, S. Sangodoyin, S. Hur, J. Park, J. Zhang, and A. F. Molisch, "Stationarity region of Mm-Wave channel based on outdoor microcellular measurements at 28 GHz," in *2017 IEEE Mil. Comm. Conf. (MILCOM)*, Oct 2017, pp. 782–787.

[11] Z. Cui, Z. Zhong, K. Guan, and D. He, "An Acceleration Method for Ray-Tracing Simulation Based on Channel Quasi-Stationarity Regions," in *12th European Conf. on Ant. and Prop. (EuCAP 2018)*, April 2018, pp. 1–5.

[12] J. Klemme, P. Varutti, B. Sander, F. Niemann, and T. Szczepanski, "Simulation Software for Radio Wave Propagation in V2X-applications," in *European Conf. on Smart Objects, Syst. and Tech. (Smart SysTech 2019)*, 2019, pp. 1–9.

[13] F. Hossain, T. K. Geok, T. A. Rahman, M. N. Hindia, K. Dimyati, C. P. Tso, and M. N. Kamaruddin, "A smart 3D RT method: Indoor radio wave propagation modelling at 28 GHz," *Symmetry*, vol. 11, no. 4, p. 510, Apr. 2019.

[14] T. K. Geok, F. Hossain, and A. T. W. Chiat, "A novel 3D ray launching technique for radio propagation prediction in indoor environments," *PLoS ONE*, vol. 13, no. 8, Aug 2018.

[15] F. Fuschini, M. Zoli, E. M. Vitucci, M. Barbiroli, and V. Degli-Esposti, "A Study on Millimeter-Wave Multiuser Directional Beamforming Based on Measurements and Ray Tracing Simulations," *IEEE Trans. on Ant. and Prop.*, vol. 67, no. 4, pp. 2633–2644, Apr. 2019.

[16] F. A. Rodríguez-Corbo, L. Azpilicueta, M. Celaya-Echarri, R. M. Shubair, and F. Falcone, "Mmwave channel stationarity analysis of v2x communications in an urban environment," *IEEE Ant. and Wireless Prop. Letters*, pp. 1–5, 2023.

[17] L. Azpilicueta, P. Lopez-Iturri, J. Zuñiga-Mejia, M. Celaya-Echarri, F. A. Rodríguez-Corbo, C. Vargas-Rosales, E. Aguirre, D. G. Michelson, and F. Falcone, "Fifth-Generation (5G) mmWave Spatial Channel Characterization for Urban Environments' System Analysis," *Sensors*, vol. 20, no. 18, p. 5360, sep 2020.

[18] L. Azpilicueta, M. Rawat, K. Rawat, F. M. Ghannouchi, and F. Falcone, "A ray launching-neural network approach for radio wave propagation analysis in complex indoor environments," *IEEE Trans. on Ant. and Prop.*, vol. 62, no. 5, pp. 2777–2786, 2014.

[19] F. A. Rodríguez-Corbo, L. Azpilicueta, M. Celaya-Echarri, P. Lopez-Iturri, I. Picallo, F. Falcone, and A. V. Alejos, "Deterministic 3D Ray-Launching Millimeter Wave Channel Characterization for Vehicular Communications in Urban Environments," *Sensors*, vol. 20, no. 18, p. 5284, Sep. 2020.

[20] F. A. Rodríguez-Corbo, L. Azpilicueta, M. Celaya-Echarri, P. Lopez-Iturri, A. V. Alejos, R. M. Shubair, and F. Falcone, "Deterministic and Empirical Approach for Millimeter-Wave Complex Outdoor Smart Parking Solution Deployments," *Sensors*, vol. 21, no. 12, p. 4112, Jun 2021.

[21] M. Yang, B. Ai, R. He, Z. Ma, Z. Zhong, J. Wang, L. Pei, Y. Li, J. Li, and N. Wang, "Non-Stationary Vehicular Channel Characterization in Complicated Scenarios," *IEEE Trans. on Veh. Tech.*, vol. 70, no. 9, pp. 8387–8400, Sep. 2021.